

SWAN EVALUATION IN THE NORTHERN GULF OF MEXICO

James D. Dykes, Y. Larry Hsu and W. Erick Rogers

Oceanography Division, Naval Research Laboratory
Stennis Space Center, MS 39529
E-mail: dykes@nrlssc.navy.mil

1. INTRODUCTION

SWAN (Simulating Waves Nearshore, Booij et al., 1999) is a wave model that can be run at high resolution in the littoral regions of the ocean and shows promise to provide output within the practical limits driven by operational constraints. Domains covering denied locations of operational interest afford little opportunity to thoroughly test and evaluate model results. To build confidence in the model results and meet the new demands of preparing SWAN for operational use, SWAN testing and evaluation is being undertaken as part of the Northern Gulf of Mexico Littoral Initiative (NGLI, Asper et al., 2001; Carroll and Szczechowski, 2001). The NGLI Project provides an ideal venue for the experimentation of an operational SWAN implementation within an extensive observing system in predominantly shallow water. The SWAN domain is set up in the Mississippi Bight to take advantage of this observing network and study the model behaviour in an isolated environment where there exist less complicated wave conditions resulting from multiple weather events.

SWAN is a third generation numerical wind wave model with shallow water physics. Since the model can be configured to run with different physics and source term specifications, model control parameters have been adjusted in various ways to determine its sensitivities by analyzing comparisons between model output and buoy observations. In this paper a local wind wave event in August and September 2000 is studied with variable model control parameters for the source terms. A particularly interesting swell event in January 2001 is investigated to see how well SWAN models such conditions. To verify the model's performance, results from runs using National Data Buoy Center (NDBC) buoy spectral information at the outer boundary of the SWAN domain is compared to results from runs using output spectra from the latest version of the Wave Model (a. k. a. WAM Cycle 4, Koman et al., 1994) run at the Naval Oceanographic Office (NAVOCEANO). Model wind forcing is provided by output from the Coupled Ocean/Atmosphere Mesoscale Prediction System (COAMPS, Hodur and Doyle, 1998) run at Fleet Numerical Meteorology and Oceanography Center.

2. OVERVIEW OF DOMAIN

2.1 Observation Network

The location of the wave sensors in the NGLI area of study is illustrated in Figure 1, and their particulars are listed on Table I. Buoy 42042 is the experimental research buoy. Each of the three NDBC directional wave buoys used for model validation are 3-meter discus buoys with an on board Datawell Hippy 40, which measures buoy heave acceleration, pitch angle, and roll angle. Wave measurements provided by NDBC buoys, including directional wave measurements, enjoy a reputation for high quality. The wave measurement sampling period consists of three separate periods: a 40-minute period for capturing long waves, a 20-minute period for intermediate waves, and a 10-minute period for short waves.

TABLE I
Locations and Depths of NDBC Stations

NDBC Buoy	Longitude		Depth (m)
	Latitude (°N)	(°W)	
42007	30.1000	88.7800	13.4
42040	29.2000	88.2500	238
42042	29.8917	88.3208	35

2.2 General Model Setup

This implementation of SWAN in the Mississippi Bight has been well established (Hsu et al., 2000). In this study, the latest version, 40.11, is setup to run in the non-stationary mode at a 12-minute time step. The domain first discussed in this paper is

the outlined box in Figure 14. This area is rotated (18° counterclockwise) aligning the southern boundary so that the outer boundary is parallel to the bathymetry contours. In this way wave data from buoy 42040 can be used as input at the deep water boundary. This configuration is not meant to be implemented operationally.

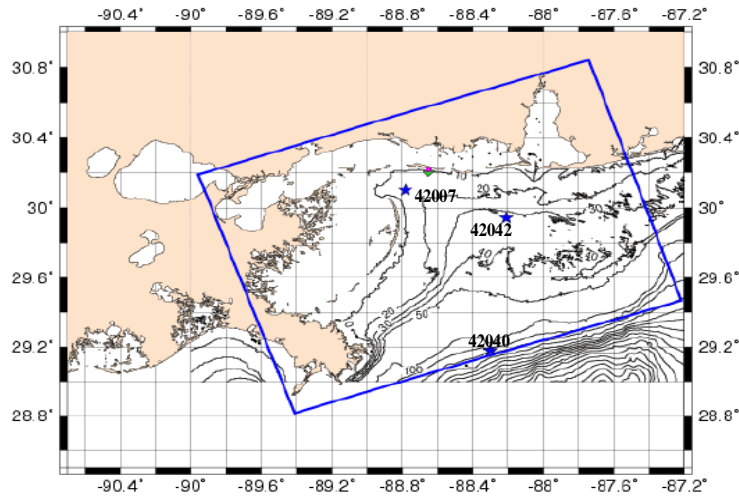


Figure 1. NGLI depths in meters and locations of NDBC buoys. The outlined box delineates the larger SWAN domain.

The input bathymetry resolution is one kilometer which is the same as that of the computational grid. The input wind grid is the COAMPS 12-minute resolution grid of winds vectors. WAM, which provides modelled deep water spectral input, runs as a nest within a series of nests, graduating from the global one degree to the 5-minute resolution nests. These nests are still run operationally at NAVOCEANO. Spectral output files for various locations around the SWAN domain have been saved. All inputs are arranged to run in hindcast mode, i. e. inputs are TAUs 0, 3, 6, 9, 0, etc.

These SWAN model runs were set up to use the backward space, backward time propagation scheme, was initialized with its default initial conditions, and used dissipation from whitecapping by Komen (1984). Unless otherwise noted, the default bottom friction (JONSWAP, Hasselmann et al., 1973) is used.

3. MODEL EVALUATION OF TWO CASES

TABLE II
Error Statistics of SWAN Runs vs. NDBC at Stations 42042 and 42007

		42042	42007
H_s (m)	N	166	155
	R	0.86	0.87
	RMS	0.30	0.24
	M	0.71	0.82
T_{avg} (s)	B	0.03	0.00
	R	0.74	0.58
	RMS	0.61	0.72
	M	0.68	0.71
θ_{avg} (°N)	B	1.69	0.21
	R	0.58	0.71
	RMS	34.8	21.3
	M	1.10	0.77
	B	-44.7	31.4

3.1 Wind Wave Case Evaluation

In this case SWAN was run for the period 28 August - 19 September 2000. For this period WAM and COAMPS were evaluated in a companion paper (Hsu et al., 2002), and their results give high confidence that SWAN's performance would not be adversely affected by the WAM input. This section gives the results of the comparison between NDBC buoy measurements of significant wave height, H_s ; average wave period, T_{avg} ; and average wave direction, θ_{avg} ; and SWAN model output. According to Table II, there is reasonably good agreement

between model output and observations. Significant wave height RMS error is as low as 0.24 metres. The scatter plots of model versus observations are shown in Figure 2; time series are also included. In Table II, R is the linear correlation coefficient between the model estimates and measurements. M is the slope of the linear regression curve through the set of model-measurement pairs. B is the y-intercept of that linear regression curve.

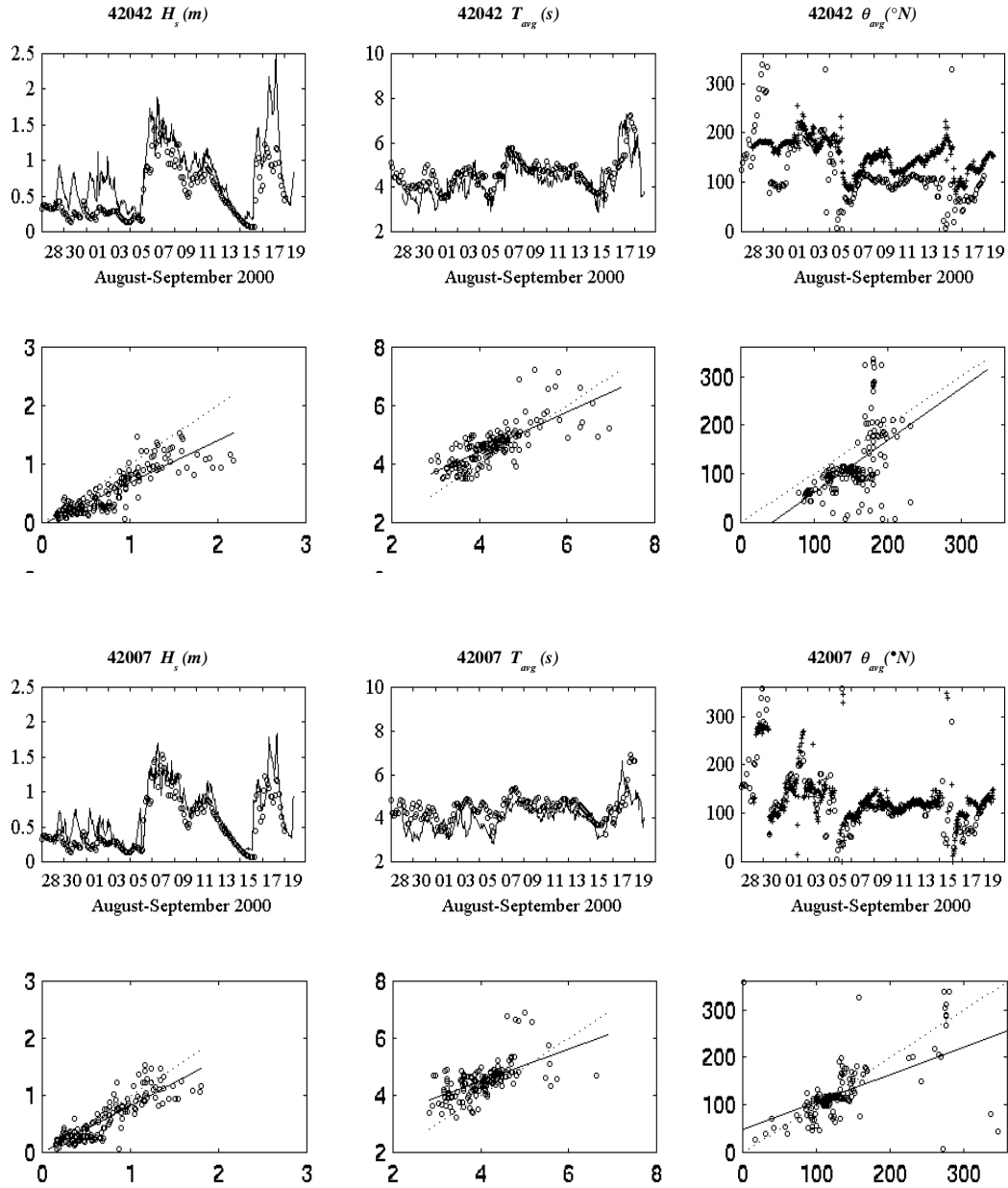


Figure 2. Time series of SWAN estimates and NDBC measurements for wave parameters at the buoy locations indicated. Scatter plots are model versus measurements where the solid line is the best fitted linear regression line and the dotted line is has a slope of unity and a y-intercept of zero.

3.2 Parameter Selection of Wind Wave Case

3.2.1 Frequency Range

In SWAN, the user can select the range and resolution for frequency. Because of the rarity of extremely long swells, the lowest frequency is set at 0.06. The high limit of SWAN is 1 Hz whereas the high frequency cutoff for most NDBC buoys is at 0.35 Hz. This frequency cutoff is related to buoy response to waves. In the Mississippi Bight, especially in the Sound, short waves are often present. Therefore, it is useful to examine the effect of calculating the bulk parameter with high frequency cutoff. A comparison of wave height and mean period between full range, i. e. cutoff at 1 Hz and cutoff at 0.35 Hz is shown in Figures 3 and 4. It is evident from Figure 3 that the

wave height increases resulting from extending to 1 Hz is small. But, the difference in mean wave period is significant, due to the definition of mean period, which is weighted by frequency. Note that in both SWAN simulations, the model is run with the highest frequency (1 Hz), but the bulk parameter is simply calculated from the SWAN output using different cutoffs.

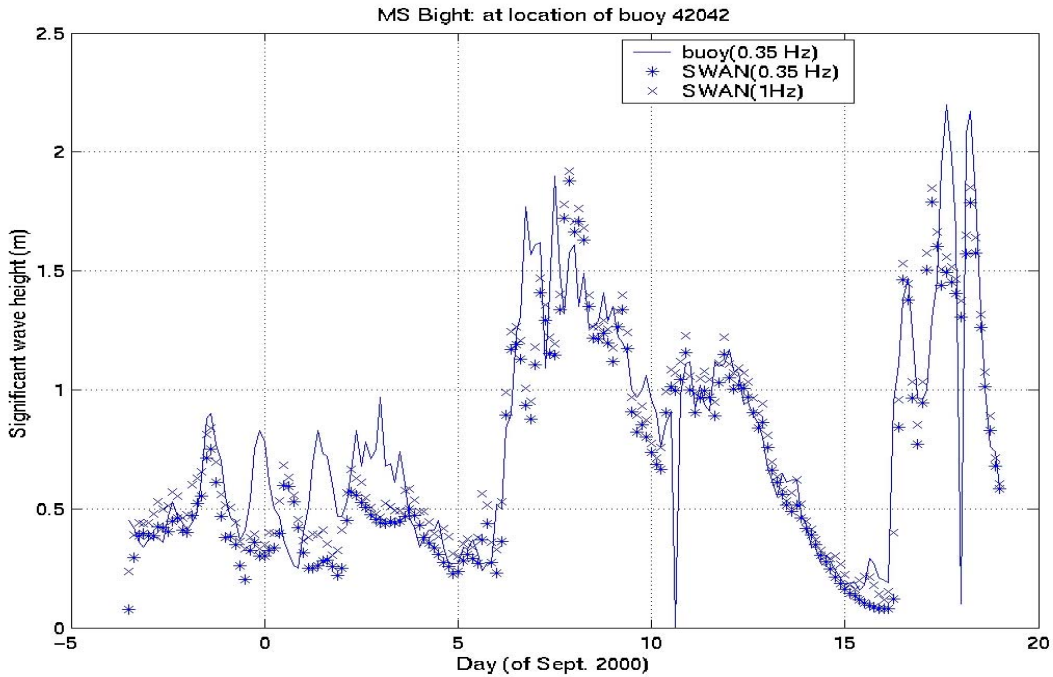


Figure 3. Comparison of mean wave period between frequency cutoff at 0.35 Hz and 1 Hz.

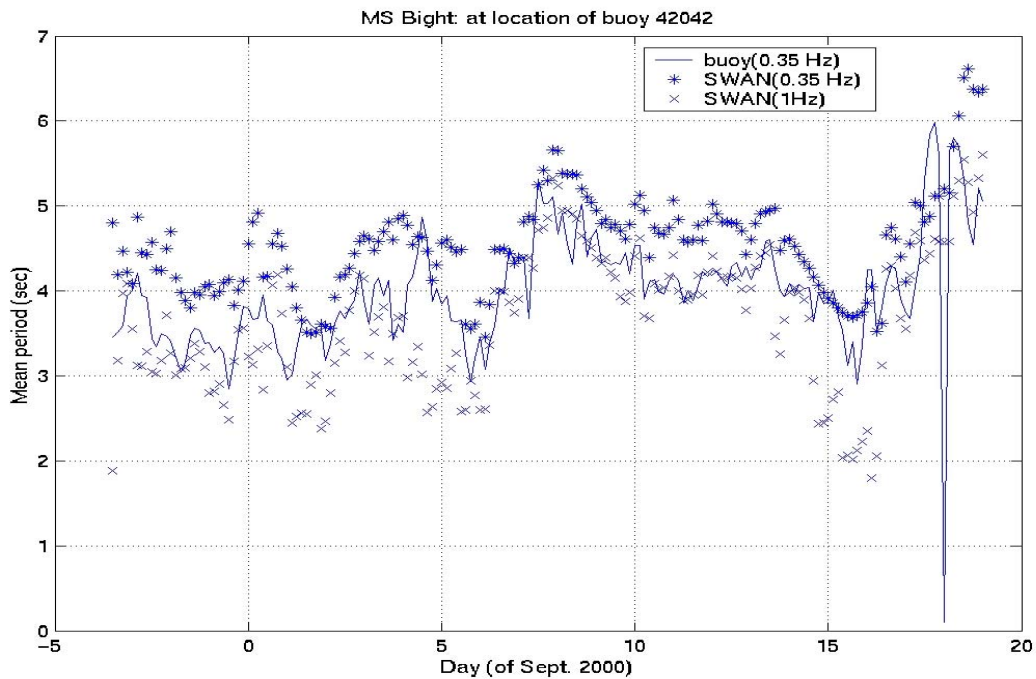


Figure 4. Comparison of mean wave period between frequency cutoff at 0.35 Hz and 1 Hz.

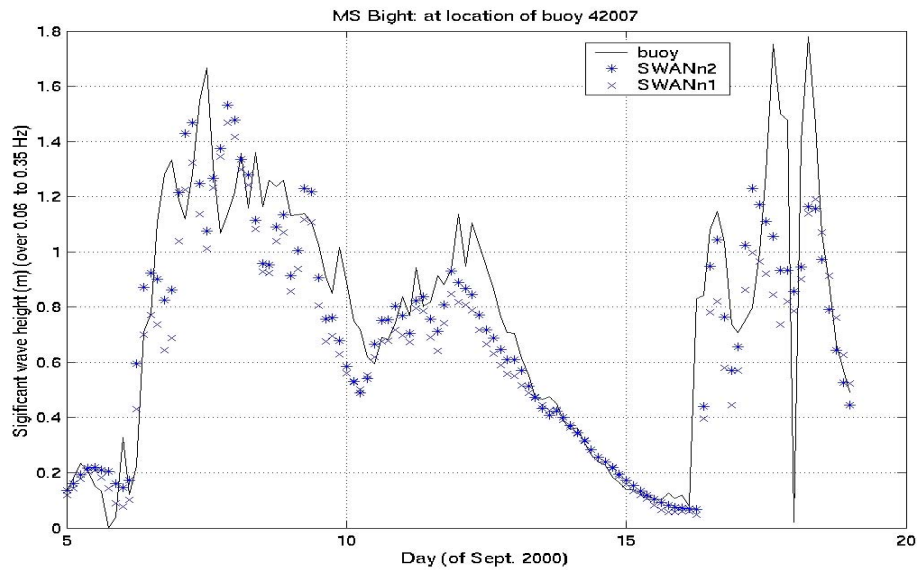


Figure 5. Wave height comparison between dissipation parameter values of 1 and 2.

3.2.2 Whiting Dissipation

Whiting is primarily controlled by wave steepness. It not only affects the shape of the wave spectra, but also growth rate of wave generation. The dissipation function is proportional to $(k/k_m)^n$ where k is the wave number, k_m is the mean wave number and n is a free or empirical parameter. In their previous study, Rogers et al. (2002) suggested that n value of 2 gives better results than the default of 1. Both significant wave height and mean period between values of 1 and 2 are compared in Figures 5 and 6. The results of n value of 2 agree better with the data. A sample comparison of spectral shape for 9 September is shown in Figure 7. The case for n value of 2 produces less high frequency energy and much better agreement with data at lower frequencies.

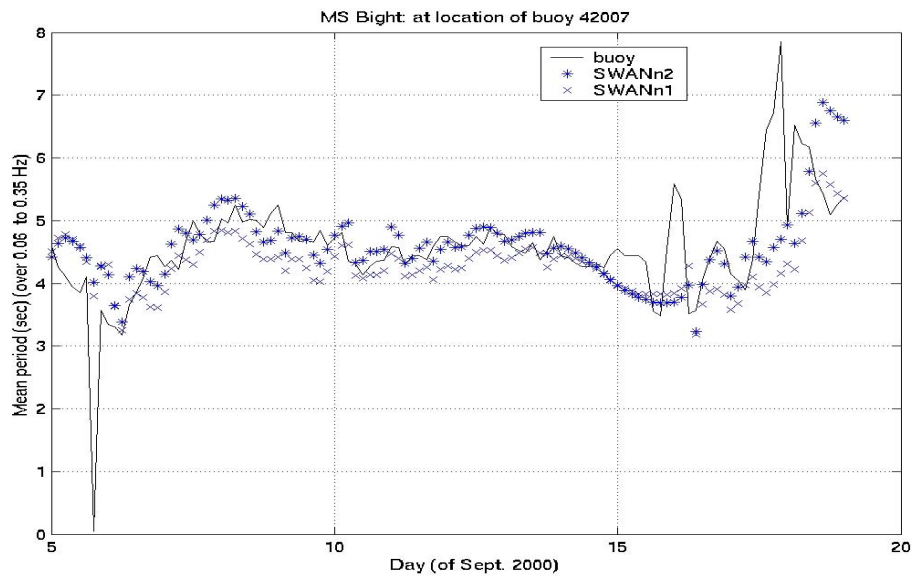


Figure 6. Wave period comparison between dissipation parameters of 1 and 2.

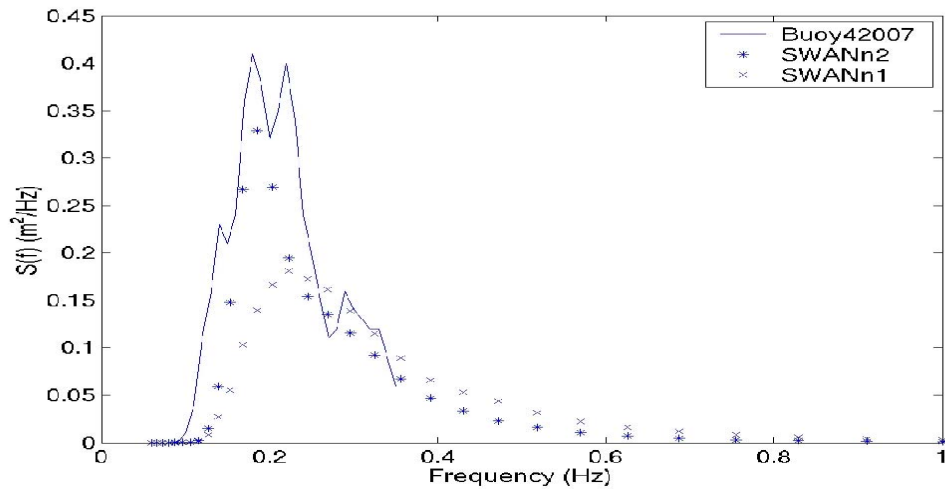


Figure 7. Spectral comparison between buoy measurements and SWAN using dissipation parameters of 1 and 2.

3.2.3 Effect of Bottom Friction

SWAN incorporates several bottom friction options. The default is the semi-empirical expression derived from the JONSWAP results by Hasselmann et al. (1973). The recommended friction coefficients are 0.067 for wind wave conditions, and 0.038 for swell. However, SWAN offers no option for a combined wave and swell condition. The comparison between cases with and without bottom friction using the default value of 0.067 is shown in Figure 8. The substantial drop for the case with bottom friction indicates that waves are over-dissipated. A calibration for bottom friction is beyond the scope of this paper. It requires much longer record and choice of wave direction. At present, SWAN is slightly under-predicting the waves, so including bottom friction is not a critical issue at least for offshore areas outside of the islands. Inside the Sound, bottom friction should be included, but a careful selection of friction scheme and coefficient is required.

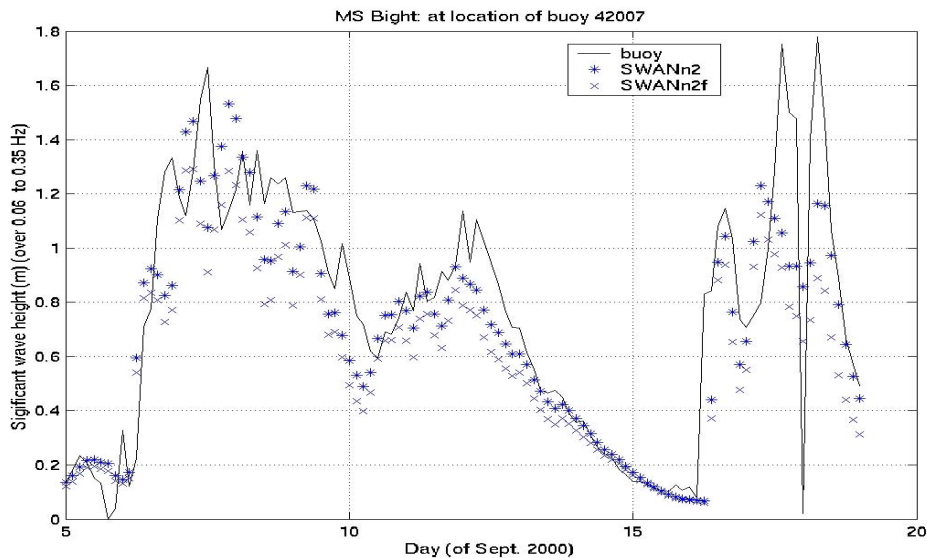


Figure 8. Wave height comparison between buoy measurements and cases with (SWANn2f) and without (SWANn2) bottom friction

3.3 Swell Event Case

Towards the end of the wind case there occurred a swell event during which SWAN did not perform well. The WAM results as reported by Hsu et al. (2002) showed that WAM was late in the arrival of swell waves and in the beginning completely missed an 11-second swell. This could impact SWAN's performance which depends heavily on the accuracy of WAM input. Detailed investigation of the swell event was hindered by the failure of buoy 42040, therefore there was not enough data to be conclusive. Even so, there was still an indication of a model performance trend in swell events in this regime worth further investigation.

To assure that SWAN can perform when given accurate input, a case in a new time frame was selected on 18 - 21 January 2001. Spectral data from buoy 42040 was made available for SWAN input. The buoy data was converted to directional spectra by the maximum likelihood method (MLM, Earle et al., 1999). In this case spectra was set up to represent the energy for the entire southern boundary in lieu of all the WAM spectral input points used before. The side boundaries could be ignored due to the orientation of incoming energy which is predominantly from the southeast. Given the results from previous experiments, an empirical parameter controlling the dissipation due to whitecapping was set to 2. Results from SWAN driven by buoy and by WAM input are compared with each other and the observation at buoy 42007.

Clearly Figure 9 shows that WAM energy is delayed when compared to reported energy at the deep water boundary. By 1400 UTC 19 January the buoy reports increasing significant wave height whilst it is not until 1800 UTC that the event starts in WAM, a six hour lag time, during which differences as much as 1.2 metres. But, this effect was not so apparent at the shallow water buoy. Figure 10 shows that results from the SWAN runs are similar throughout. Besides minor detectable perturbations, results from both SWAN runs essentially agreed with the observations regardless of the difference in input.

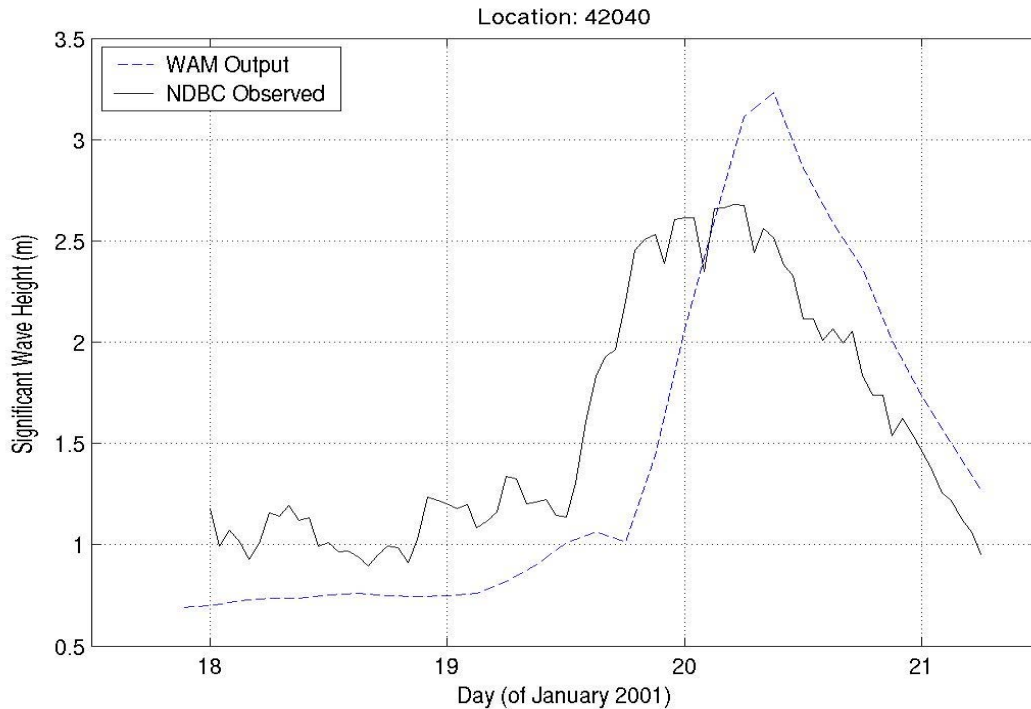


Figure 9. Time series of significant wave height from WAM and observation at NDBC Buoy 42040.

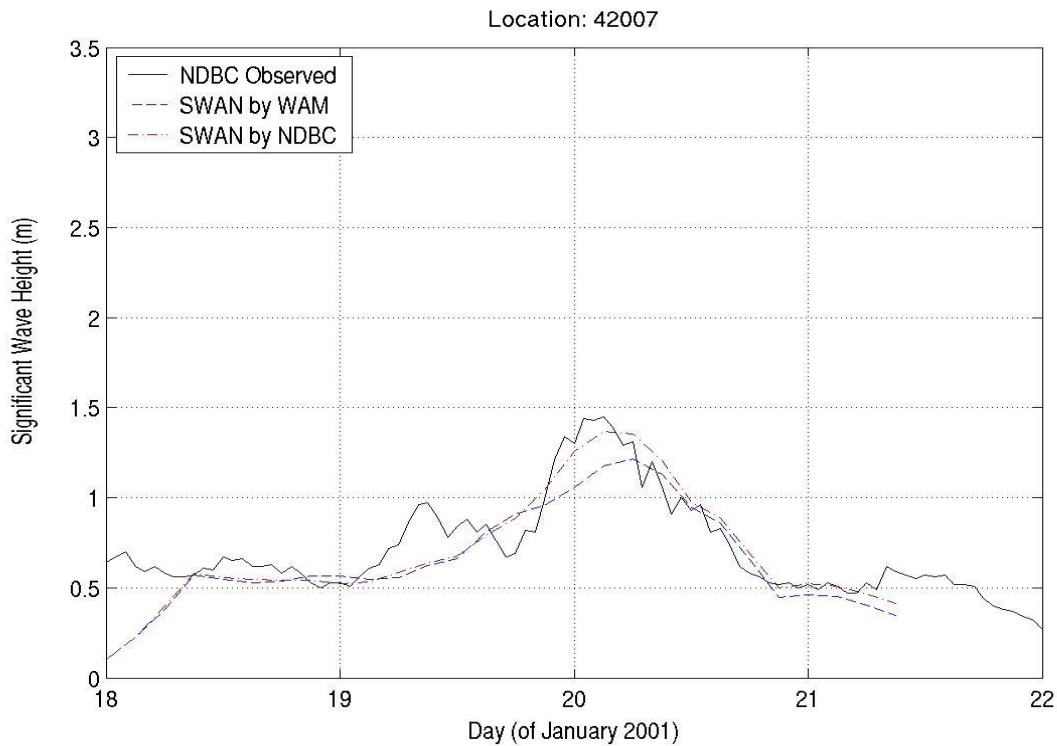


Figure 10. Time series of significant wave height from WAM and observation at NDBC Buoy 42007.

To gain further understanding, we need to look at the frequency spectra at both buoy locations. Figure 11 shows buoy and WAM output frequency spectra for 19 January 2001 21 UTC at which time it is apparent that according to the buoy the wave energy is mostly attributed to swell with peak period around ten seconds. Swell from WAM output was much smaller compared to the spectra of the deep water buoy. To account for the time of wave propagation from the boundary to this location, the data for 20 January 00 UTC was selected for comparison. Figure 12 shows the SWAN spectra output compared to measurements. The energy density at the peak frequency for swell from buoy 42040 is decreased by an order of magnitude upon arrival at 42007 accounting for a decrease of significant wave height from 2.5 metres to 1.3. SWAN driven by the deep water buoy was able to represent a similar occurrence. There is no swell to speak of according to the SWAN driven by WAM input. Thus, wave heights from locally generated waves account for nearly all the energy, whose peak agrees fairly well with the observed.

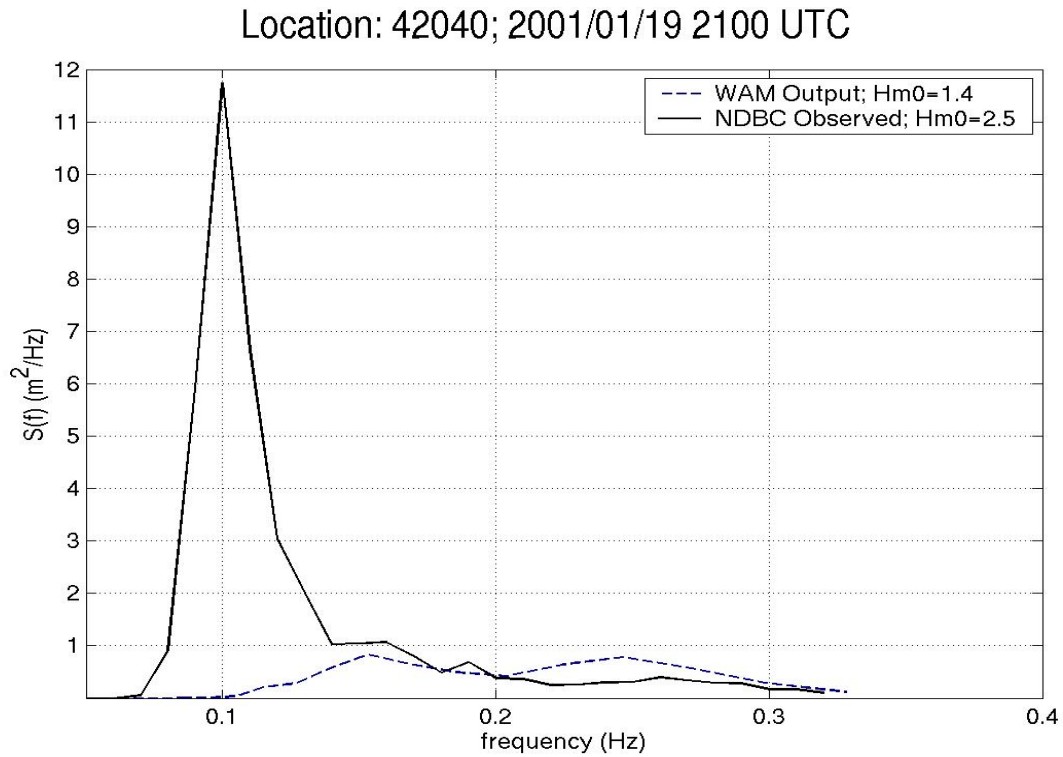


Figure 11. Frequency spectra of WAM output and NDBC buoy measurements at the deep water boundary of the SWAN domain. $Hm0$ represents significant wave height in metres.

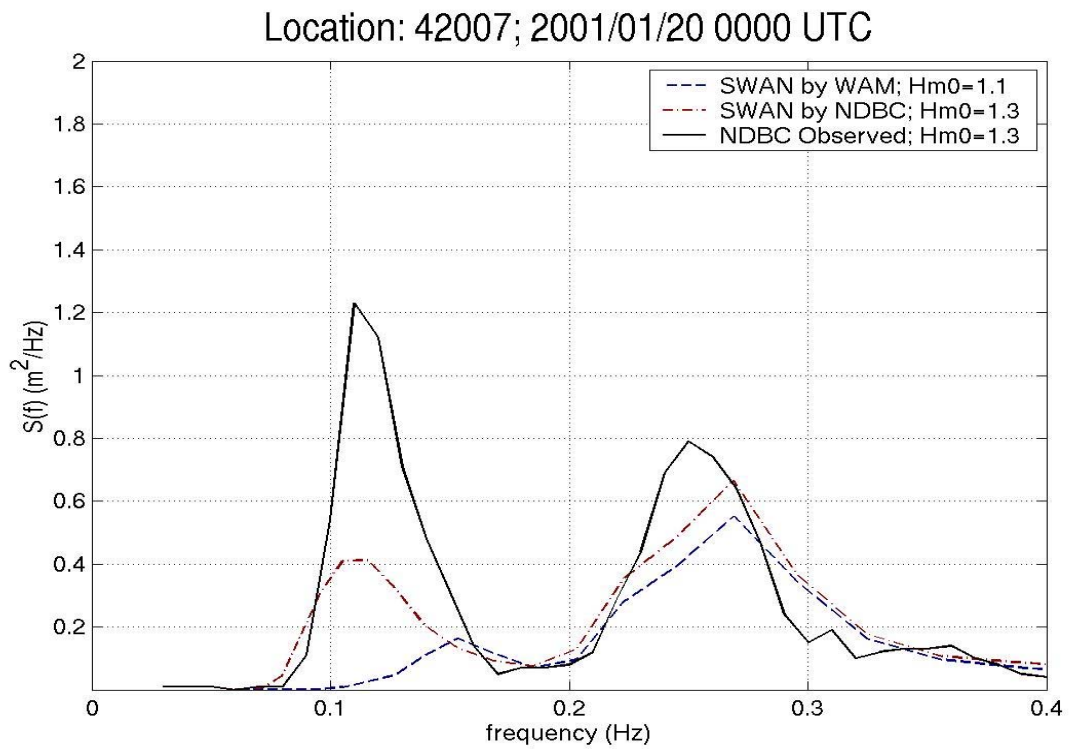


Figure 12. Frequency spectra of SWAN output and NDBC buoy measurements at a point well within the model domain. $Hm0$ represents significant wave height in metres.

Much of the energy at the deep water boundary had been moving towards the northwest along a trough axis of bathymetry. The shallow water buoy location is situated towards the other end of the axis. A reasonable explanation why so little swell energy reaches that buoy is the refraction of the long waves to either side of the trough axis.

4. CONCLUSION

The analysis of two representative cases helped us examine the performance of SWAN in handling wind waves and swell. Due to ideal experimental conditions of the NGLI, these cases could be isolated. In either case it is shown that SWAN performs well given good input winds from COAMPS and boundary spectra from WAM. The wind wave case aided in determining better parameter selection. The swell case increased our understanding of the behaviour of swell in the Mississippi Bight.

Several operational issues remain to be considered. The primary goal from an operational perspective is to be able to obtain reasonably accurate wave forecasts in minimal time. Clearly, a reduction in the resolution in time, space and spectral parameters would cut overall time, but more studies are needed to determine the optimal cuts. In many cases, a small enough domain set up to run in stationary mode would provide good forecasts in little time (Dykes, et al., 2002). Also being addressed is the goal of effectively coupling SWAN to a host wave model such as WAM (Wakeham et al., 2002). With the switch from high performance supercomputers to more portable systems the issue whether to use boundary condition files straight from WAM or WaveWatch III (Tolman, 1990; Tolman and Chalikov, 1996) or spectral point files created when the host is done is still important. In addition, the issues regarding how SWAN should be parallelized, either with shared or distributed memory techniques, must be explored.

ACKNOWLEDGEMENTS

NAVOCEANO through the NGLI program manager, Dr. John Blaha, provided major funding for the measurement and validation efforts. Part of the efforts in wave model evaluation is funded under PE 63207N and sponsored by Space and Naval Warfare Systems Command (SPAWAR) under Coastal Wave and Surf Model project. The SPAWAR manager is Mr. Tom Piowar. Dr. David Wang within the Naval Research Laboratory kindly provided the MLM software.

REFERENCES

- Asper, P., J. Blaha, C. Szczechowski, C. Cumbee, R. Willems, S. Lohrenz, D. Redalje, and A-R. Diercks, 2001: The Northern Gulf of Mexico Littoral Initiative (NGLI): A collaborative modeling, monitoring, and research effort. *J. Miss. Acad. Sci.*, Vol. 46, No. 1, 60.
- Booij, N., R. C. Ris and L. H. Holthuijsen, 1999, A third-generation wave model for coastal regions, Part I, Model description and validation. *J. Geoph. Research*, C4, 104, 7649-7666.
- Carroll, S. N. and C. Szczechowski, 2001: The Northern Gulf of Mexico Littoral Initiative. In: *Proc. MTS/IEEE Oceans 2002*, Honolulu, Hawai'i, 1311-1317.
- Dykes, J. D., Y. L. Hsu, and W. E. Rogers, 2002: The Development of an Operational SWAN Model for NGLI. Submitted to: *Proc. MTS/IEEE Oceans 2002*, Biloxi, Mississippi.
- Earle M. D., K. E. Steele, and D. W. C. Wang, 1999: Use of advanced directional wave spectra analysis methods. *Ocean Engineering*, 26 (12), 1421-1434.
- Hasselmann, K. and coauthors, 1973, Measurements of wind wave growth and swell decay during the Joint North Sea Project (JONSWAP). *Dtsch. Hydrogr. Z. Suppl.*, 12, A8.
- Hodur, R. M., and J. D. Doyle, 1998: The coupled ocean/atmosphere mesoscale model prediction system (COAMPS). *Coastal Ocean Prediction, Coastal and Estuarine Studies* 56, 125-155.
- Hsu, Y. L., W. E. Rogers, J. D. Dykes, 2002: WAM performance in the Gulf of Mexico with COAMPS wind.

Submitted to: *Proc. 7th International Workshop on Wave Hindcasting and Forecasting*, Banff, Alberta, Canada.

Hsu, Y. L., W. E. Rogers, J. M. Kaihatu, and R. A. Allard, 2000: Application of SWAN in Mississippi Sound. In: *Proc. of 6th International Workshop on Wave Hindcasting and Forecasting*, Monterey, CA, 398-403.

Komen, G. J., S. Hasselmann, and K. Hasselmann, 1984: On the existence of a fully developed windsea spectrum, *J. Phys. Oceanogr.*, 14, 1271-1285

Komen, G. J., Cavaleri, L., Donelan, M., Hasselmann, K., Hasselmann, S. and P. A. E. M. Janssen, 1994: *Dynamics and Modelling of Ocean Waves*, Cambridge University Press, 532 p.

Rogers, W. R., P. A. Hwang and D. W. C. Wang, 2002, Investigation of wave growth and decay in the SWAN model: three regional-scale applications, *J. of Physical Oceanography*, accepted for publication.

Tolman, H. L., 1990: Wind wave propagation in tidal seas. Doctoral thesis, Delft Univ. of Tech., also Comm. Hydr. Geotech. Eng., Delft Univ. of Tech., report 901-, 135p.

Tolman, H. and D. Chalikov, 1996: Source terms in a third generation wind wave model, *J. Phys. Oceanogr.*, Vol 26, 2497-2518.

Wakeham, D., R. Allard, J. Christiansen, T. Taxon, S. Williams, 2002: The Distributed Integrated Ocean Prediction System. Submitted to: *Proc. 7th International Workshop on Wave Hindcasting and Forecasting*, Banff, Alberta, Canada.

WAMDI Group, 1988: The WAM model-a third-generation ocean wave prediction model. *J. Phys. Oceanogr.*, 18, 1775-1810.